

Optimization of LY545694 Tosylate Controlled Release Tablets Through Pharmacoscintigraphy

Evelyn D. Lobo · Mark D. Argentine · David C. Sperry · Alyson Connor · John McDermott · Lloyd Stevens · Ahmad Almaya

Received: 28 February 2012 / Accepted: 29 May 2012 / Published online: 14 June 2012
© Springer Science+Business Media, LLC 2012

ABSTRACT

Purpose To optimize a controlled release (CR) matrix formulation with two goals: (1) effectively deliver a prodrug to a preferred absorption region of the upper GI tract, and (2) afford a PK profile similar to a “reference” CR formulation.

Methods A pharmacoscintigraphic clinical study was conducted using a flexible formulation design space. A six-arm, three-prototype study was employed to cover the formulation design space and assess performance against the reference formulation. Pharmacokinetic and scintigraphic data from the first three dosing arms were used to select prototypes to be dosed in subsequent arms.

Results Of three prototypes tested, the third prototype had an optimal release rate. The *in vivo* erosion rate was observed via scintigraphy to reach 90% in 3 h. The AUC ratio relative to the reference for the prodrug was 1.25, while the C_{\max} ratio was 1.07. The ratios for the active moiety were 1.31 (AUC) and 1.01 (C_{\max}).

Conclusions A single pharmacoscintigraphic study efficiently investigated a wide formulation design space and precisely optimized the release rate with few formulation iterations. The selected formulation provided the desired exposure at a 30% lower dose. The approach is beneficial when drug absorption is limited to a region of the GI tract.

KEY WORDS absorption · controlled-release · flexible design space · pharmacokinetics · prodrug

INTRODUCTION

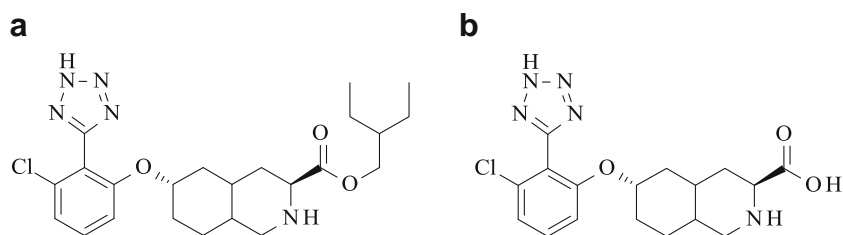
LY545694 is an ester prodrug that is primarily hydrolyzed by carboxyesterases (present in the small intestine, blood, and liver) to the active moiety, Compound 645838, a potent and selective ionotropic glutamate receptor antagonist identified as a potential treatment for the management of persistent pain. The structures of each compound are illustrated in Fig. 1. Due to the low permeability of Compound 645838, LY545694 was developed to enhance the oral bioavailability and systemic exposure of Compound 645838. The solubility of LY545694 is ~0.4–0.8 mg/mL across the physiologic pH, with two pK_a values at approximately 3.5 and 8.6. Initial Phase 1 studies of LY545694 as immediate-release formulations (solution and capsules) indicated a short terminal half-life for LY545694 (mean range: 0.72 to 4.5 h) and Compound 645838 (mean range: 2 to 3 h). Dose-limiting adverse events were gastrointestinal (GI) related symptoms such as loss of appetite, nausea, and vomiting. The timing of the adverse events suggested that they might be associated with the maximum plasma concentration of either LY545694 and/or Compound 645838 (mean range of t_{\max} : 0.67 to 3 h). Given the desire to modify the concentration-time profile of LY545694 and Compound 645838 to reduce C_{\max} and provide the targeted exposure for an extended period of time that would permit a once or twice daily dosing regimen, controlled release (CR) formulations were investigated.

Initial efforts investigated LY545694 CR tablet formulations having the same dosage strength but exhibiting three different *in vitro* release rates: fast, intermediate, and slow release to achieve 80% release in 3, 8–10, and 14 h, respectively. A pharmacokinetic (PK) study in healthy volunteers with these 3 CR formulations demonstrated that the CR formulations allowed for a twice-daily dosing regimen of

E. D. Lobo · M. D. Argentine · D. C. Sperry · A. Almaya (✉)
Eli Lilly and Company
Indianapolis, Indiana, USA
e-mail: almaya_ahmad@lilly.com

A. Connor · J. McDermott · L. Stevens
Quotient Clinical Limited
Nottingham, United Kingdom

Fig. 1 Structures for (a) the LY545694 prodrug and (b) the Compound 645838 active metabolite. Note: Tosylate counterions not shown.



LY545694 with an acceptable concentration-time profile for Compound 645838. The CR formulation with the intermediate release profile was selected to support the subsequent Phase 1 and 2 studies because it provided reasonable drug exposure with reduced C_{\max} and peak-to-trough ratio. These attributes were anticipated to improve the side-effect profile observed following oral administration of LY545694.

Deconvolution was conducted in parallel with Phase 1 and 2 clinical safety and efficacy studies, which utilized the selected intermediate release CR formulation. Importantly, the *in vivo* absorption profile indicated that the absorption period was limited, as LY545694 absorption for all 3 CR formulations stopped at approximately 6 h post-dose. Based on expected GI transit times for a tablet formulation administered in the fasted state, this would equate to absorption occurring throughout the small intestine and into the proximal colon (1). Further, the cumulative amount of LY545694 absorbed was significantly higher for the fastest-releasing formulation compared with the slowest-releasing formulation. These findings suggested that the intermediate release formulation may not be optimal as a significant fraction of the dose may be released outside the region available for absorption, thus passing through the GI tract unabsorbed. As a result, variations in GI motility may lead to variability in the fraction of the absorbed dose, which may have an impact on the adverse-event profile and may create the need for dose adjustments. These results suggested the need for further formulation development to optimize the composition of the CR formulation such that the *in vivo* release rate would approximate delivery within the small intestine. Earlier studies indicated that cumulative drug input into the body was impacted by the formulation release rate, which meant that adjustments to both dose as well as release rate might be required in order to optimize the formulations and maintain comparability of the PK profiles.

An *in vivo* formulation optimization clinical study was designed to identify an optimal CR formulation by investigating formulations with various compositions and *in vitro* release rates. Performance of these formulations in humans was used to select an optimal formulation composition for which the release *in vivo* approximated delivery within

the small intestine. To maximize flexibility and precision, a design space concept was planned, in which regulatory approval was achieved for a continuous formulation design space rather than for discrete numbers of pre-defined, pre-characterised systems. Assessment of *in vivo* performance was not limited to PK data, but was also evaluated by the assessment of *in vivo* GI transit and erosion of the CR tablets. Such assessment was possible through the use of gamma scintigraphy, where a radiolabeled carrier is incorporated within the CR tablets during tablet manufacture.

The technique of gamma scintigraphy was first used to investigate the *in vivo* release properties of drug formulations in 1976 and has become an increasingly useful tool for evaluating the GI performance of pharmaceutical dosage forms (2–4). Gamma scintigraphy has been used in the development and evaluation of pharmaceutical drug delivery systems, including enteric-coated tablets and complex modified release formulations (5–7). The technique provides information on the deposition, dispersion, and movement of a formulation. Typically, such scintigraphic imaging is combined with measurement of drug concentrations in blood or urine to provide information concerning the sites of release and absorption (termed pharmacoscintigraphy) within the body (8–11).

As will be shown, by utilizing the flexible design space approach, a single study can simultaneously explore a wide range of release rates and precisely define an optimal release rate. This is possible because emerging data from each arm of the study are used to make real time decisions concerning which regions of the design space to focus on for subsequent dosing arms. Furthermore, concomitant scintigraphic data enable a more direct measure of *in vivo* drug release rate and anatomical location than typical PK methods alone. Scintigraphic data are helpful to both explain unexpected PK observations and to elucidate complexities resulting from absorption that is limited to the small intestine and proximal colon, and often complicated by patient variability. Principally, these two aspects make the study described in this manuscript the most efficient method to develop a CR formulation for this compound.

This manuscript presents the results of the *in vivo* formulation optimization study using pharmacoscintigraphy

in an adaptive design to identify an optimal CR formulation for LY545694 tosylate. The optimal formulation was targeted to have a release profile within the small intestine and achieve a plasma concentration-time profile comparable to the existing Phase 2 formulation (reference CR formulation) using a lower dose. While pharmacoscintigraphy is not novel nor is the approach toward evaluation of CR formulations, the novelty of this approach involved a single, relatively small clinical study to effectively optimize a CR formulation within a seven-week clinical timeframe.

MATERIALS AND METHODS

Dosage Forms

Six dosage forms were investigated in the clinical study as described in Table I. The solution formulation was manufactured at Quotient Clinical (Nottingham, UK) and contained the equivalent of 25 mg LY545694 delivered in degassed Sprite® (172 mL, 18.9 g sugar and 70 kcal per dose) to provide a taste mask. It is unlikely that the caloric load of this formulation would result in any significant modification of the gastric emptying time. The total caloric load was less than half of what has been shown to cause some impact on motility (12). The unlabeled reference CR formulation containing the equivalent of 35 mg LY545694 was manufactured by Eli Lilly and Company (Indianapolis, IN, USA).

All CR formulations radiolabeled with ≤ 1 MBq indium-111 (^{111}In) were manufactured at Quotient Clinical. The reference CR formulation (35 mg strength) was prepared using a bulk intermediate LY545694 powder blend containing Methocel® K4M Premium CR, LY545694 tosylate, lactose, colloidal silicon dioxide, and magnesium stearate. Indium-111 radiolabeled resin has been routinely applied in the literature for the radiolabeling of oral formulations (13–15). The radioactive resin was prepared by exchanging ^{111}In ions onto the surface of an insoluble cationic exchange resin (Amberlite IRP69, sodium polystyrene sulfonate USP, Rohm and Haas) using a dilute ^{111}In chloride solution.

Table I Dosage Forms Tested in the Clinical Study

Dosing period	LY545694 (mg)	Formulation	Radiolabel
1	25	Oral solution	n/a
2	25	CR - Prototype 1	^{111}In
3	35	CR - Reference	^{111}In
Interim analyses			
4	25	CR - Prototype 2	^{111}In
5	25	CR - Prototype 3	^{111}In
6	35	CR - Reference	n/a

The mixture was evaporated to dryness and the resultant ^{111}In radiolabeled resin was recovered. Aliquots (400 mg) of the drug powder blend were hand-blended with ^{111}In radiolabeled ion exchange resin (~5 mg) using a microspatula immediately prior to tablet compression using a single station Carver tablet press (10 mm round standard concave tooling, 2000 lbs compression force, 12–18kp hardness).

The prototype CR formulations (25 mg strength) were prepared using bulk intermediate LY545694 powder blend containing Methocel® K100LV Premium CR, LY545694 tosylate, lactose, colloidal silicon dioxide, microcrystalline cellulose, and magnesium stearate. Aliquots (200 mg) of this blend were hand-blended with ^{111}In radiolabeled ion exchange resin (~3.5 mg) using a microspatula immediately prior to tablet compression using a single station Carver tablet press (8 mm round standard concave tooling, 1250 lbs compression force, 6–10kp hardness). The new prototypes contained a lower dose (25 mg LY545694) than the reference CR formulation (35 mg LY545694) because of the anticipated improvement in exposure for the prototypes as a result of the *in vivo* release rate optimization.

A single dimension design space was used in this study. The rate of drug release was controlled by amending the amount of Methocel® K100LV in the composition of the prototype CR formulations. The outer limits of the design space were defined by a low polymer extreme (fastest release profile) and a high polymer extreme (slowest release profile) containing 40 mg (20% *w/w*) and 100 mg (50% *w/w*) Methocel® K100LV, respectively. The boundaries of the design space (i.e., fastest and slowest release rates) were defined using available data (Fig. 2, curves a and e). The fastest-releasing formulation in the design space approximated the fastest release rate CR formulation previously tested and proven safe in humans. The slowest-releasing formulation approximated the *in vitro* release profile of the current reference formulation. Within the design space, a formulation

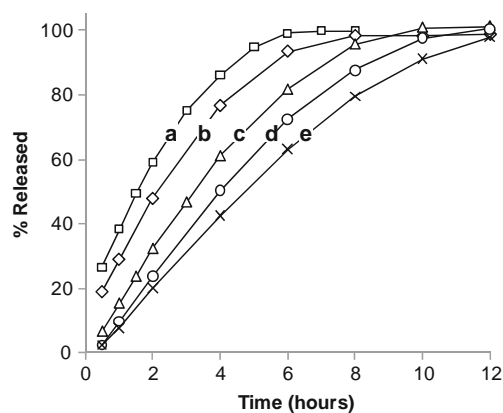


Fig. 2 Average *in vitro* drug release ($n=6$) for formulations covering the design space. Curves a-e represent five potential CR formulations that span the design space from the fastest-releasing formulation (curve a) to the slowest releasing formulation (curve e).

approximately in the middle of that space containing 30% *w/w* Methocel® K100LV was predicted to be the desired prototype and was designated as Prototype 1 (Fig. 2, curve c). The study was designed so that PK data for the solution formulation, the radiolabeled reference and Prototype 1 plus the scintigraphic data for the radiolabeled reference and Prototype 1 were evaluated in an interim analysis and the results were used to determine the composition of subsequent prototypes (Prototype 2 and 3). As Prototype 1 was approximately in the middle of the design space, additional formulations were available so that Prototypes 2 and 3 could be selected to be faster or slower releasing than Prototype 1 (Fig. 2, curves b and d). As described later in the Results and Discussion sections, PK and scintigraphy data indicated the need to test faster releasing formulations in response to Prototype 1 data. Thus, in this study, Prototypes 2 and 3 were manufactured to release faster than Prototype 1 (tablets contained 24% and 20% of Methocel® K100LV, respectively).

During development, unlabeled and cold-labeled (i.e., tablets containing non-radiolabeled ion-exchange resin) batches of the CR tablet formulations (reference and prototype formulations at the boundaries of the design space) were prepared and assessed for appearance, assay, blend uniformity, weight, breaking force, and dissolution. These data were submitted to the UK regulatory authorities to support the Chemistry, Manufacturing, and Control aspects of the Clinical Trial Application.

Following confirmation of satisfactory processes, radiolabeled batches were prepared and assessed against the same acceptance criteria. This pharmaceutical development work confirmed the acceptability of the radiolabeled tablet formulations for use in the clinical study.

Dissolution Testing

In vitro testing was performed using a USP Apparatus I (basket) configuration at 100 RPM with 900 mL of de-aerated 0.01N HCl as the dissolution medium (at 37°C). Samples were withdrawn at several time points during the dissolution test, filtered with 10 µm filters (Varian, Full Flow) and analyzed by isocratic HPLC on an ACE 3 Phenyl column with UV detection at 285 nm. The method was suitably validated for specificity, linearity, precision, accuracy, and solution stability to support the varied formulations used in this study. A dissolution medium consisting of 0.01N HCl was utilized to eliminate hydrolytic drug degradation at more neutral pH during the dissolution test. Since HPMC is non-ionic and the solubility of the compound is relatively flat across the physiologic pH range, pH is not believed to impact *in vivo* drug release. During development of the dissolution test, *in vitro* data covering the

physiologic pH range showed that medium pH did not have a significant impact on the release rate.

In some dissolution experiments, release of the ¹¹¹In radiolabel was measured by periodically stopping the dissolution test, withdrawing the remaining portion of the radioactive tablet from the dissolution vessel and assaying (Capintec CRC-15R dose calibrator) for radioactive content and correcting for decay, R_t . The percent of radioactivity released, R , was then calculated using equation 1 and the measured tablet radioactivity at the beginning of the dissolution test, R_0 .

$$R = \left(1 - \frac{R_t}{R_0}\right) \times 100 \quad (1)$$

Since this methodology requires the dissolution test to be terminated at the time point at which the sample is extracted, a complete radioactivity release profile was reconstructed using multiple samples - one sample for each time point.

Clinical Study Design

The study was conducted at Quotient Clinical (Nottingham, UK) in accordance with the Clinical Protocol, with the Declaration of Helsinki (amended Seoul, October 2008), with the International Conference on Harmonization Good Clinical Practice (ICH GCP) Guidelines, and in accordance with all applicable regulatory requirements.

Healthy subjects were selected by the investigators based on their medical history, physical examination, electrocardiograms, and routine clinical laboratory test results. Sixteen Caucasian males aged 18–65 years with a body mass index between 19 and 32 kg/m² were enrolled to have at least 10 completers. All subjects gave written informed consent for their participation.

This was an open-label, fixed treatment sequence, 6-period, single dose, crossover study design conducted at a single-center. Six different formulations, listed in Table I, were administered in a fixed sequence over 6 dosing periods. LY545694 was administered following an overnight fast (minimum 10 h) as a single oral dose. The washout period between the consecutive doses was at least 7 days.

Venous blood samples of approximately 3.5 mL were collected for the determination of plasma concentrations of LY545694 and Compound 645838. Following solution administration, blood samples were obtained at 0, 0.17, 0.33, 0.5, 0.67, 0.83, 1, 1.5, 2, 3, 4, 5, 6, 8, 12, 18, 24, 32, 48 h post-dose. Following administration of CR formulations, blood samples were collected at 0, 1, 2, 3, 4, 6, 8, 12, 16, 24, 32, 40, 48, 72 h post-dose.

Anterior and posterior planar scintigraphic images each of at least 50 s duration were acquired using a gamma camera (General Electric Maxicamera) at approximately

10 min intervals until eight hours post-dose, 30 min intervals until 12 h post-dose, and then at 16, 20, 24, 36, 48 and 72 h post-dose. Anterior and posterior exterior anatomical markers were used to facilitate the subsequent image analysis and image acquisition was performed with subjects standing.

Bioanalytical Method

Human plasma samples were analyzed for LY545694 and Compound 645838 using the validated liquid chromatography with tandem mass spectrometry (LC/MS/MS) method at Advion BioServices, Inc. (Advion, Ithaca, NY, USA). The lower limit of quantitation was 0.05 ng/mL for LY545694 and Compound 645838. The upper limit of quantitation was 5 ng/mL for both analytes. Samples above the limit of quantification were diluted and reanalyzed to yield results within the calibrated range. LY545694 and Compound 645838 in human plasma are stable for up to 146 days (Low, High, and Dilution QC) when stored at approximately -20°C and 254 days when stored at approximately -70°C .

For the initial 3-day validation, interassay accuracy (% relative error) ranged from -6.3% to -1.7% for LY545694 and from -6% to 0.2% for Compound 645838. The interassay precision (% relative standard deviation) was $\leq 8.8\%$ for LY545694 and $\leq 14.1\%$ for Compound 645838.

Pharmacokinetic Analysis

The plasma concentration-time profiles of LY545694 and Compound 645838 were analyzed using non-compartmental methods with WinNonlin Professional Edition (Pharsight Corp, Version 5.0.1). The relative bioavailability was estimated using dose normalized AUC. The maximal plasma concentration (C_{max}) and area under the concentration-time curve ($\text{AUC}_{0-\infty}$) for LY545694 and Compound 645838 were evaluated using a mixed effects analysis of variance (ANOVA) model. The C_{max} and $\text{AUC}_{0-\infty}$ were log-transformed prior to analysis. The estimate of ratios of geometric means and the corresponding 90% confidence intervals between each prototype formulation and the unlabeled reference CR formulation were calculated.

Scintigraphic Data Analysis

Scintigraphic data from the radiolabeled formulations (CR reference, Prototypes 1, 2, and 3) were analyzed by both qualitative and quantitative methods as reported previously (9).

The scintigraphic data were analyzed to obtain the following parameters: gastric emptying time, colon arrival time, anatomical location of initial radiolabel release, anatomical location of complete radiolabel release, and tablet erosion profile.

For the qualitative assessment of transit and disintegration, the time at which each of the events occurred was taken as the mid-time between the times recorded for the two consecutive images encompassing the transition. For example, gastric emptying was defined as the mid-time between the time of the last image in which the tablet was still located in the stomach and the time of the next image in which the tablet was present in the small intestine. Initial tablet erosion was defined as the time to detect any sign of release of radioactive marker from the tablet. Complete tablet erosion was defined as the time at which all the radiolabeled marker had dispersed in the GI tract and no signs of a distinct core remained. The possible anatomical locations for initial and complete tablet erosion were stomach (S), proximal small bowel (PSB), distal small bowel (DSB), ascending colon (AC), hepatic flexure (HF), transverse colon (TC), splenic flexure (SF), and descending colon (DC).

Quantitative scintigraphic analysis of tablet erosion was performed using a custom-written program (Quotient Clinical) using Micas X Plus Software. Results were expressed as the amount of radiolabel remaining in the tablet as a percentage of initial radiolabel and the time at which 10%, 50% and 90% erosion ($t_{10\%}$, $t_{50\%}$, $t_{90\%}$) had occurred. Data were corrected for radioactive decay, background radiation and tissue attenuation.

Scintigraphic data were correlated with pharmacokinetic data by the production of scatter plots. Trends were identified by observation. No formal assessment of correlation was performed.

RESULTS

Dissolution Results

Several CR formulations were developed to define the design space for this study, and their *in vitro* dissolution profiles are shown in Fig. 2. The initial formulation, defined as Prototype 1, was approximately in the middle of the design space and released 80% in ~ 6 h (curve c), while the fastest and slowest formulations in the design space released 80% in ~ 3.5 h and ~ 8 h, respectively (curves a and e). The reference CR formulation released 80% of the drug in ~ 10 h.

The *in vitro* release characteristics for both LY545694 and radioactivity for the fastest and slowest formulations in the design space as well as for the reference formulation are shown in Fig. 3. The release profile of ^{111}In (detected as radioactivity) was similar to the drug release profile. Importantly, these data confirm that measuring release of radioactivity is a suitable surrogate for measuring drug release in these formulations.

The release rates of the 3 prototype CR formulations used in the clinical study (Fig. 4) were as expected based on

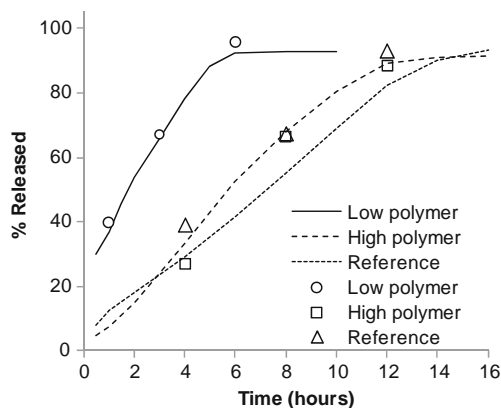


Fig. 3 *In vitro* drug release (lines) and radioactivity release (symbols) profiles to illustrate comparable radioactive release as a surrogate for drug release. Six tablets for each lot were tested. Each radioactivity release data point is the result from one tablet removed from the set of six. With three radioactivity data points, three tablets remained at the end of the test to measure drug release.

formulation development across the design space. Note that drug release reached a plateau at ~95% for all formulations. This was a result of a specific interaction between LY545694 and the radiolabel carrier, Amberlite IRP-69. IRP-69 is a pharmacopeial ion exchange resin (sodium polystyrene sulfonate USP) used to bind cationic substances including drugs. Since LY545694 is charged in the low pH of the dissolution medium, some of the drug was bound to the resin and consequently not released into solution during *in vitro* testing.

Pharmacokinetic Results

Sixteen healthy male subjects participated and 12 out of the 16 subjects completed all the periods of the study. The mean (range) age was 34 years (21 to 44 years) and mean body weight was 76.5 kg (56 to 100 kg).

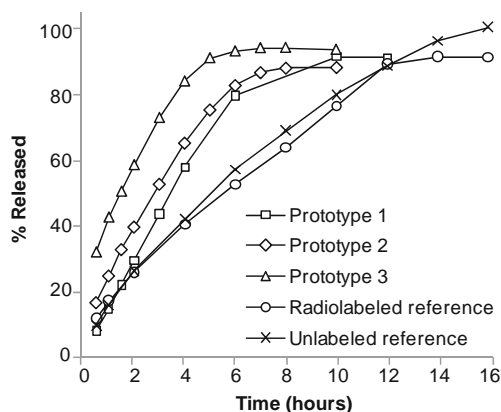


Fig. 4 *In vitro* dissolution profile of CR dosage forms tested in the clinical study. Radiolabeled reference and unlabeled: $n=12$, Prototypes 1, 2 and 3: $n=6$.

The summary of the PK parameters for all formulations are shown in Table II. As expected, the solution formulation was characterized by a much higher C_{max} and shorter t_{max} , relative to all of the CR formulations.

The mean plasma concentration-time profiles for LY545694 and Compound 645838 following the 35 mg radiolabeled reference CR formulation were similar to that of the 35 mg unlabeled LY545694 reference CR formulation (Fig. 5, Table II). The geometric mean ratio (radiolabeled/unlabeled formulation) of AUC and C_{max} ranged from 0.92 to 1.03 and the 90% CI ranged from 0.71 to 1.30.

Based on the *in vitro* dissolution profiles of the prototypes, the rank order with regard to dissolution rates was (slowest to fastest): Prototype 1 > Prototype 2 > Prototype 3 (Fig. 4). Consistent with this trend, following single oral-dose administration of the prototype formulations in the fasted state, the time course of both LY545694 and Compound 645838 resulted in C_{max} and AUC progressively increasing for Prototype 1 to Prototype 3 (Fig. 6, Table II).

Among the three prototypes, Prototype 3 (25 mg) provided a concentration-time profile for LY545694 and Compound 645838 most comparable to that observed with the reference CR formulation (35 mg), (Fig. 6). However, the C_{max}/C_{12h} ratio of Compound 645838 (Table II), which was used as a surrogate for peak-to-trough ratio at steady state was highest with Prototype 3 and approximately 19% higher than that observed with the reference CR formulation. The relative bioavailability (dose-normalized AUC) of Compound 645838 relative to reference CR formulation suggests that bioavailability with Prototype 3 was approximately 30% higher than the reference CR formulation. Prototypes 1 and 2 appear to be bioequivalent to the reference CR formulation as the relative bioavailability was nearly one and was contained within the 90% confidence interval (CI). The C_{max} ratio for LY545694 and Compound 645838 with Prototype 3 (25 mg) relative to reference CR formulation (35 mg) was close to one. The mean relative bioavailability (*versus* solution) of the unlabeled CR formulation and Prototype 3 for LY545694 was 1.15 and 1.44, respectively and for Compound 645838 the values were 0.54 and 0.71, respectively.

Scintigraphic Results

The results of the GI transit time analysis for the radiolabeled CR reference and the prototype formulations are provided in Table III. Gastric emptying and colon arrival were only reported if the tablet remained intact or had only partially eroded while in the stomach or small intestine, respectively. On average, gastric emptying and colon arrival times were all as expected following administration in the fasted condition regardless of the formulation. Although the reference CR formulation tablet (400 mg tablet weight, 10 mm diameter) was larger than the prototype tablets (200 mg tablet weight,

Table II Pharmacokinetic Parameters for Solution, CR Reference and Prototypes 1, 2, and 3

Parameters	Solution	Unlabeled Reference	Radiolabeled Reference	Prototype 1	Prototype 2	Prototype 3
Dose (mg)	25	35	35	25	25	25
N	16	14	16	16	15	15
t_{max} (h)	0.51 (0.33–2.00)	3.00 (2.00–4.00)	3.16 (1.00–4.00)	3.00 (2.00–4.03)	3.00 (2.00–4.12)	3.00 (2.00–4.07)
C_{max} (ng/mL)	134 (27)	65.6 (57)	71.6 (39)	47.2 (39)	60.6 (42)	70.3 (40)
AUC (ng.h/mL)	173 (44)	280 (46)	300 (47)	205 (36)	230 (38)	249 (29)
C_{max}/C_{12h}	465 (79.4)	23.8 (52.2)	24.8 (67)	25.2 (59)	32.8 (51)	49.9(90.6)
C_{max} ratio (90% CI)	–	–	0.92 (0.71, 1.18)	0.72 (0.57, 0.91)	0.92 (0.73, 1.16)	1.07 (0.85, 1.35)
^a AUC Ratio (90% CI)	–	–	0.93 (0.73, 1.20)	1.02 (0.82, 1.29)	1.15 (0.92, 1.45)	1.25 (0.99, 1.56)
t_{max} (h)	1.75 (1.50–4.00)	4.00 (4.00–6.00)	4.00 (3.00–6.00)	4.00 (2.00–6.00)	4.00 (3.00–6.03)	4.00 (3.00–6.00)
C_{max} (ng/mL)	130 (19)	70.5 (28)	68.7 (50)	47.1 (50)	52.9 (43)	71.3 (37)
AUC (ng.h/mL)	687 (22)	521 (29)	556 (45)	356 (44)	395 (44)	488 (35)
C_{max}/C_{12h}	16.9 (30.2)	6.07 (3.1)	4.87 (39)	5.72 (32)	6.12 (30.3)	7.23 (44)
C_{max} ratio (90% CI)	–	–	1.03 (0.81, 1.30)	0.67 (0.54, 0.83)	0.75 (0.60, 0.94)	1.01 (0.81, 1.26)
^a AUC Ratio (90% CI)	–	–	0.94 (0.76, 1.16)	0.96 (0.78, 1.18)	1.06 (0.86, 1.31)	1.31 (1.06, 1.62)

Median (range) reported for t_{max}

Geometric mean (%CV) reported for C_{max} , AUC, C_{max}/C_{12h}

^a Dose normalized AUC ratios versus unlabeled reference

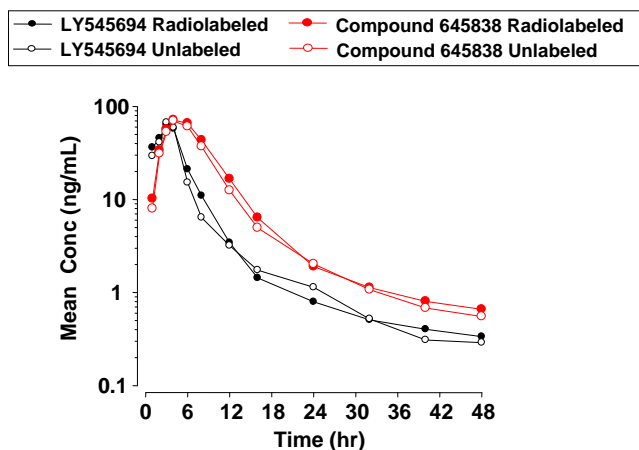


Fig. 5 Comparison of *in vivo* performance characteristics of LY545694 unlabeled and radiolabeled reference CR formulations.

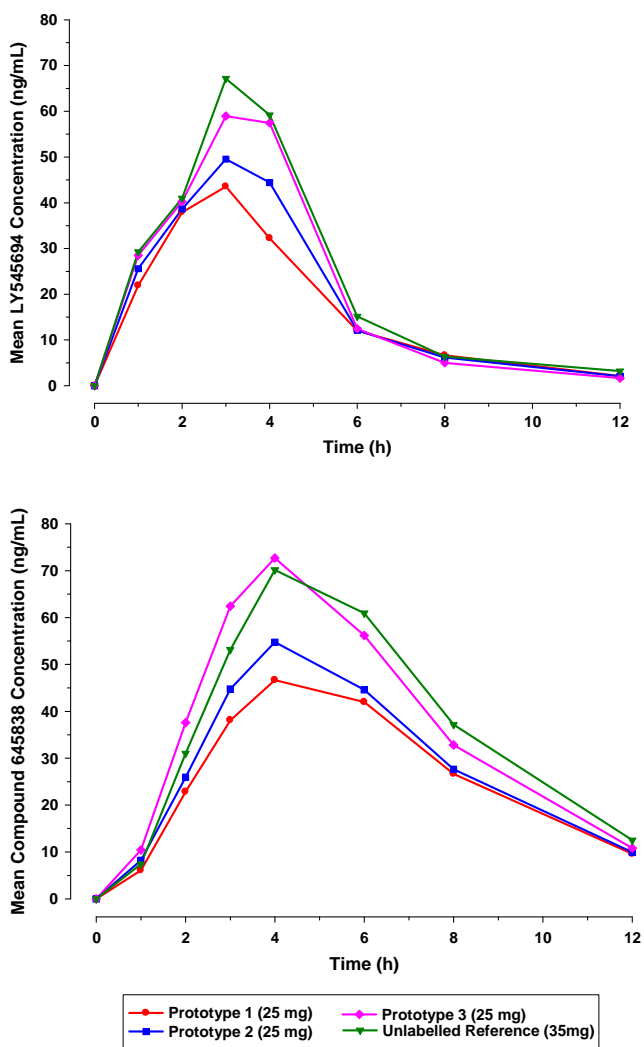


Fig. 6 Comparison of LY545694 and Compound 645838 concentration time profiles following oral administration of Reference and Prototype CR formulations.

Table III Gastrointestinal Transit Times for the Radiolabeled CR Reference and Prototype Formulations (Hours Post-Dose)

Formulation	Gastric emptying time		Colon arrival time	
	Mean (SD)	N	Mean (SD)	N
CR - reference	0.59 (0.686)	11	3.27 (0.967)	7
CR - prototype 1	0.78 (0.698)	15	3.63 (2.121)	11
CR - prototype 2	0.74 (0.786)	14	2.97 (0.883)	7
CR - prototype 3	0.87 (0.887)	13	3.12 (0.617)	3

8 mm diameter), this difference had no effect on gastric emptying. For all radiolabeled formulations investigated, fewer subjects have reported colon arrival times compared to the number of reported gastric emptying times because often complete tablet erosion occurred before the formulation reached the colon. Among the prototypes, the number of subjects for which colon arrival was observed is as follows: Prototype 1 > Prototype 2 > Prototype 3; which is consistent with the progressively increasing dissolution rate of the prototypes.

Among the prototype formulations, Prototype 1 eroded more distally in the GI tract than Prototype 2, which eroded more distally than Prototype 3 (Fig. 7). The location of complete erosion was variable for the radiolabeled CR reference formulation ranging from the stomach to the SF. Contrary to expectations based on the *in vitro* data, in many subjects complete erosion of the radiolabeled reference CR formulation occurred earlier than observed for Prototype 1.

The results of quantitative assessment of tablet erosion are provided in Fig. 8 and Table IV. Data for $t_{10\%}$ and $t_{90\%}$ are reported, representing the quantitative assessment of onset and completion of tablet erosion. Data for $t_{50\%}$ were reviewed, but are not reported here. The radiolabeled CR reference formulation and Prototype 1 had similar times for onset of erosion, as indicated by the mean $t_{10\%}$ values (Table IV). Initial erosion times ($t_{10\%}$) for Prototypes 2 and 3 were also similar, but slightly faster than the other two formulations. However, complete erosion times did illustrate differences which can be seen from the mean $t_{90\%}$ values (Table IV). Prototype 1 had the longest mean complete erosion time at 5.8 h, while Prototypes 2 and 3 eroded faster at 4.4 h and 3 h, respectively. These scintigraphic observations are consistent with the *in vitro* release rates of the formulations shown in Fig. 4. In contrast, the mean complete erosion time for the radiolabeled reference CR formulation was 4.0 h, which was shorter than recorded for Prototype 1 and did not reflect the *in vitro* release rate.

Pharmacokinetic-Scintigraphic Correlation

In order to identify relationships between key PK parameters and the *in vivo* performance of the formulations, a number of

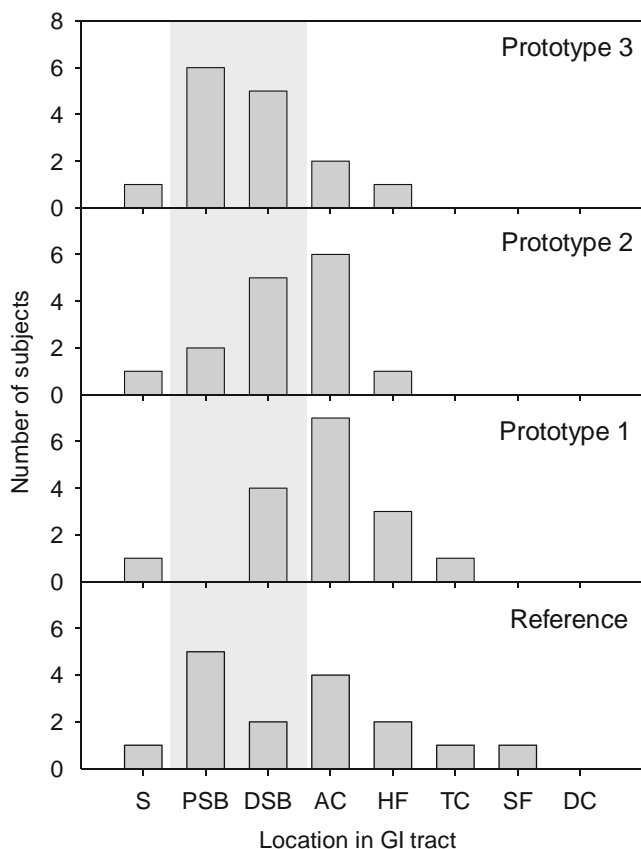


Fig. 7 Anatomical location of complete erosion for the radiolabeled reference and prototype CR formulations. The light gray shaded area indicates the apparent regions available for absorption. Figure abbreviations are as follows: stomach (S), proximal small bowel (PSB), distal small bowel (DSB), ascending colon (AC), hepatic flexure (HF), transverse colon (TC), splenic flexure (SF), and descending colon (DC).

correlations were performed. The results are provided in Figs. 9, 10 and 11. The impact of anatomical site of delivery on the LY545694 and Compound 645838 exposure was assessed by examining the correlation between the site of

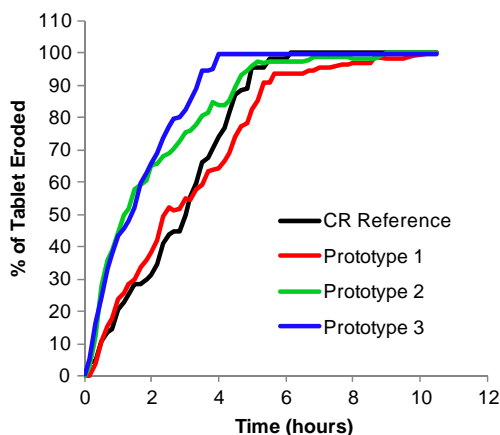


Fig. 8 Average *in-vivo* erosion profiles for each of the four radiolabeled formulations studied.

complete tablet erosion with AUC (Fig. 9). There was no discernable trend for LY545694; however, for Compound 645838 the exposure reduced as the anatomical site of complete tablet erosion became increasingly distal.

A similar correlation was performed for time taken to achieve tablet erosion ($t_{90\%}$) with AUC. Only a very limited trend was observed for the radiolabeled CR reference and prototype 1, suggesting that the longer erosion time resulted in decreased exposure. More in-depth review of the data revealed that gastrointestinal transit times were a confounding factor. In subjects with the highest exposure, the tablet remained in the proximal gastrointestinal tract (e.g., stomach) for the duration of drug release hence ensuring that delivery was to the small intestine.

The impact of the rate of GI transit on exposure can be observed by comparing gastric emptying time with AUC (Fig. 10). Those subjects with more rapid transit into the small intestine (shorter time to gastric emptying) exhibited reduced extent of absorption, particularly for Compound 645838. Subjects in whom the dosage form remained in the stomach for a longer period of time exhibited absorption at the higher end of the observed range.

An assessment of anatomical site of delivery on the conversion of prodrug to the active moiety (metabolite to parent ratio, MTP(%)) was also performed. The results are provided in Fig. 11 and suggest that conversion to Compound 645838 may be influenced by site of delivery, with conversion reduced as the site becomes more distal.

DISCUSSION

The primary objective of this study was the identification of an optimal CR formulation with release performance that matched the apparent absorption region throughout the small intestine (i.e., absorption over approximately 5–6 h post-dose). Gamma scintigraphy was sought to provide complementary insight into formulation performance (including verification of the hypothesized absorbance region) along with traditional PK data. Radiolabeled CR formulations were prepared and utilized to assess *in vivo* drug release and GI transit.

Prior to the execution of this study, *in vitro* data were generated to justify the use of a radiolabel for this purpose. Several articles have been published regarding release mechanisms for HPMC-based formulations (16–19), and erosion-dominated formulations had been successfully studied (20) using pharmacoscintigraphy. *In vitro* methods (17,21) that simultaneously measure hypromellose release and drug release data were utilized and results supported erosion-dominated release of the drug for the formulations used in this study. This finding justified the use of a homogeneously distributed radioactive tracer as a surrogate for drug release, since both were expected to erode and release at the same

Table IV Erosion Profiles for the Radiolabeled CR Reference and Prototype Formulations (Hours Post-Dose)

	Formulation	N	$t_{10\%}$		$t_{90\%}$	
			Mean (SD)	Range	Mean (SD)	Range
	CR - reference	16	0.71 (0.525)	0.08–2.12	4.01 (1.030)	2.22–5.88
$t_{10\%}$ - time at which 10% tablet erosion had occurred	CR - prototype 1	16	0.62 (0.389)	0.10–1.63	5.76 (1.987)	3.28–10.05
	CR - prototype 2	15	0.31 (0.222)	0.09–0.98	4.38 (1.681)	1.96–8.82
$t_{90\%}$ - time at which 90% tablet erosion had occurred	CR - prototype 3	15	0.34 (0.319)	0.11–1.36	2.98 (0.610)	1.72–3.96

rate. Indeed, radiolabeled and unlabeled formulations that were tested *in vitro* confirmed that release of radioactivity was a good surrogate for drug release (Fig. 3).

The *in vitro* dissolution data for the radiolabeled formulations plateau at ~95% released as a result of drug binding to the Amberlite™ IRP-69 resin that was used as a carrier for ^{111}In (Fig. 4). This interaction was demonstrated through *in vitro* experiments during development of the radiolabeled formulations. Potentially, the same binding effect observed *in vitro* could occur *in vivo*, limiting the availability of drug for absorption. In order to minimize this effect and the potential for *in vivo* impact, the amount of resin was limited to 3.5 mg in the prototype formulations (200 mg tablet weight) and 5 mg in the reference CR formulation (400 mg tablet weight). With this amount of resin, the amount of drug bound to the resin *in vitro* was limited to ~5%. The drug, being positively charged in the 0.01 N HCl dissolution medium, is bound to the resin by non-specific charge-charge interaction that is characteristic of ion exchange resins. Since the drug could be displaced by other positively charged species, it is likely that *in vivo* the drug is displaced from the resin by cations in the GI lumen and therefore available for absorption. *In vivo* results confirmed no appreciable resin binding effect as the C_{\max} and AUC ratios for radiolabeled and unlabeled reference CR formulations were nearly unity (Table II). Thus, both dissolution and PK results (Figs. 4 and 5) suggested that radiolabeling of the formulation with ≤ 1 MBq ^{111}In had no effect on *in vivo* performance.

A priori decision criteria were established using data from the first three dosing periods. These decision criteria were used to determine whether subsequent prototypes (Prototype 2 and 3) needed to release the drug faster or slower than Prototype 1. Relative comparison of the complete erosion time (from scintigraphy) and the absorption profile (from deconvolution) allowed the selection of subsequent prototypes. Three scenarios were possible

Scenario 1: Prototype 1 Is Acceptably Close to the Target Release Rate

If Prototype 1 *in vivo* erosion time is approximately equivalent to delivery to the small intestine, subsequent prototypes would be selected to study a region around Prototype 1.

Prototype 2 would be selected to release faster than Prototype 1 and Prototype 3 would be selected to release slower than Prototype 1 (Fig. 2, curves b and d).

Scenario 2: Need Faster Release Than Prototype 1

If Prototype 1 *in vivo* erosion time is longer and results in delivery beyond the small intestine, subsequent Prototype 2 and 3 would be faster than Prototype 1 (Fig. 2, curves b and a, respectively).

Scenario 3: Need Slower Release Than Prototype 1

This scenario would be observed if the time to reach 90% relative fraction absorbed for Prototype 1 was shorter than that for the reference CR formulation. This means that Prototype 1 is not utilizing all of the available region for absorption and slower formulations are thus needed. In this case, Prototypes 2 and 3 would be slower than Prototype 1 (Fig. 2, curves d and e, respectively).

During interim analyses, Prototype 1 had a lower AUC and a slightly lower dose-normalized AUC *versus* that of the reference CR formulation for both LY545694 and Compound 645838. These results were surprising as *in vitro* dissolution data suggested Prototype 1 was a faster-releasing formulation than the CR reference (Fig. 4). Scintigraphic data showed that for both formulations, initial erosion occurred in the stomach and an appreciable number of subjects exhibited complete erosion in the distal GI tract (colonic region), which is likely to be beyond the region available for absorption. Importantly, Prototype 1 had a mean complete erosion time that was longer than that of the reference CR formulation. Based upon the slower *in vivo* release of Prototype 1 compared to the reference CR formulation, it was determined that Prototypes 2 and 3 should both be faster-releasing than Prototype 1 (Scenario 2). Prototype 2 tablets thus contained 24% Methocel® K100LV and Prototype 3 tablets contained 20% Methocel® K100LV.

Among the prototypes, the rank order of the times for complete erosion (decreasing times) were Prototype 1 > Prototype 2 > Prototype 3 (Table IV). Overall, the complete erosion times for each formulation were consistent with the location of complete erosion (Fig. 7) such that the physical location of the tablets at the time complete erosion was more

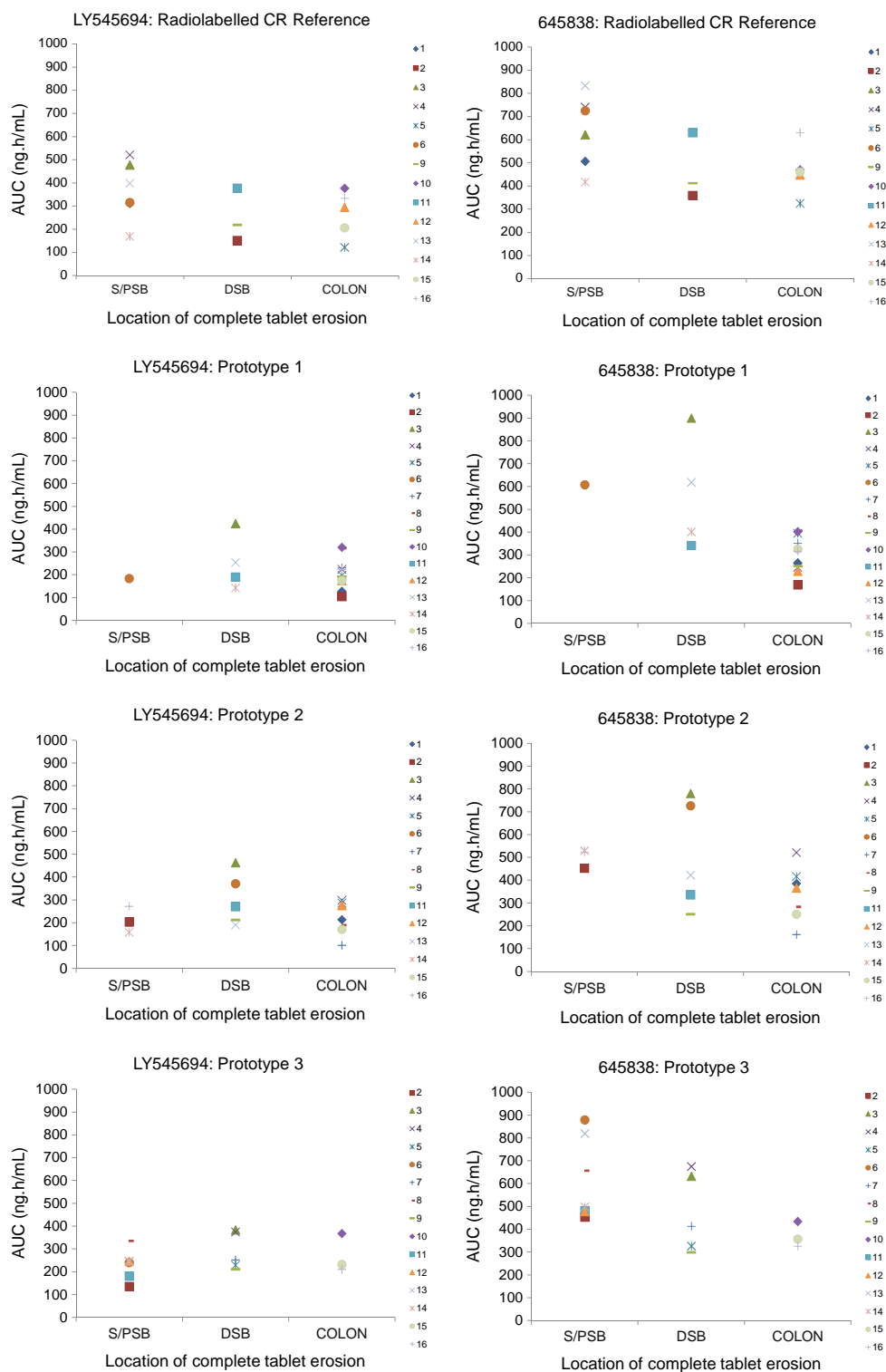


Fig. 9 Pharmacokinetic – scintigraphic correlation assessment: AUC for LY545694 or Compound 645838 versus the location for complete tablet erosion.

proximal for faster releasing prototypes. This would be expected for formulations with no significant differences in transit rates. Notably, the physical location of Prototype 3 at complete erosion showed that the tablet-release duration was consistent with the small intestine.

From a formulation composition perspective, two groups of CR tablets were utilized in this study: the prototypes and the reference CR tablets. The three investigated prototypes were similar in their physical dimensions (200 mg tablet weight, 8 mm diameter). In addition, these prototypes

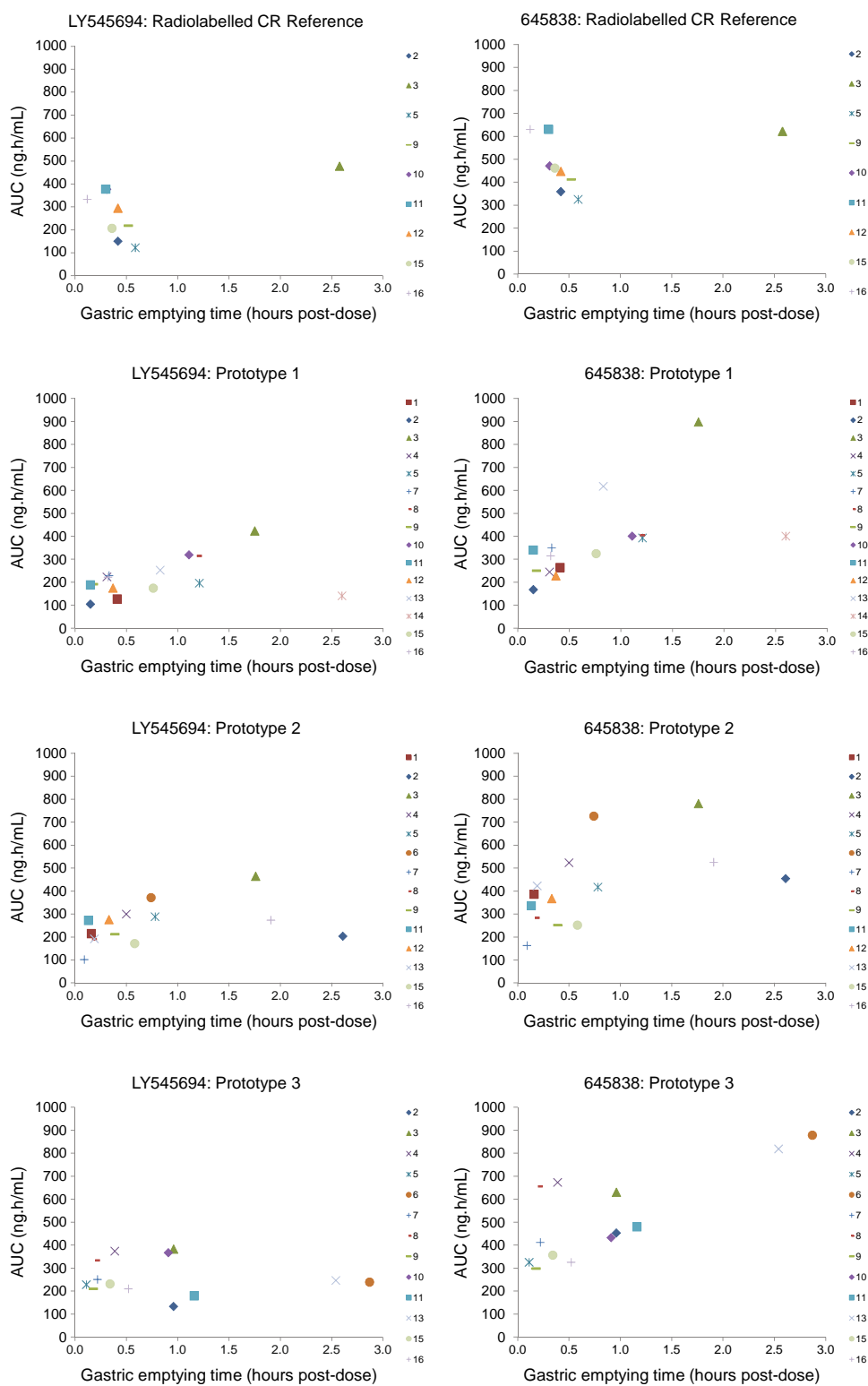


Fig. 10 Pharmacokinetic – scintigraphic correlation assessments: AUC for LY545694 or Compound 645838 versus observed gastric emptying time.

contained the same level of an insoluble filler (microcrystalline cellulose) and utilized the same grade of release-controlling polymer (K100LV Premium CR). The three prototypes only differed in their polymer content (balanced by the soluble

filler, lactose). The reference CR tablets were larger in dimension (400 mg tablet weight, 10 mm diameter), did not contain an insoluble filler, and utilized K4M Premium CR as the release-controlling polymer.

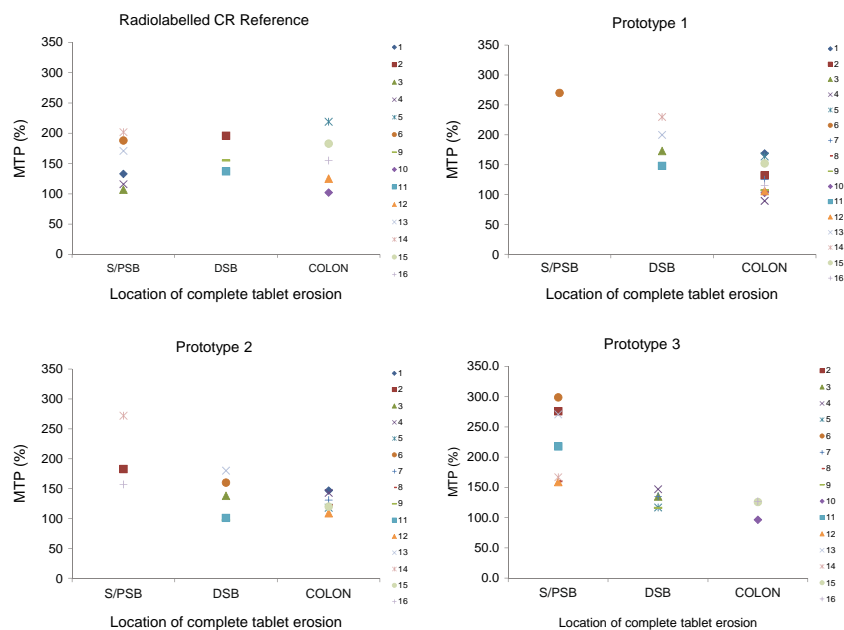


Fig. 11 Pharmacokinetic – scintigraphic correlation assessments: metabolite to parent levels (Compound 645838 to LY545694) versus the location for complete tablet erosion.

In vitro dissolution and *in vivo* scintigraphic erosion times exhibited the same relative order among the three prototypes. However, the relative release rates of the reference CR tablets compared to those of Prototype 1 were different *in vitro* compared to *in vivo*. While the *in vitro* release rate for Prototype 1 was faster than that of the reference CR formulation, *in vivo* Prototype 1 tablets eroded more slowly than reference CR tablets. Scintigraphic data clarified the underlying reasons for the differences in the *in vivo* performance of the reference CR formulation and Prototype 1. In 9 of the 16 subjects tested, loss of a distinct tablet core occurred after the reference CR tablets released $\leq 60\%$ of the radiolabeled dose. In contrast for Prototype 1, only 2 of the 16 subjects lost a distinct tablet core at this early stage of the erosion process. This indicates that the matrix of the reference CR formulation was no longer able to withstand the peristaltic contractions within the GI tract. This behavior was not observed during *in vitro* dissolution testing and clearly highlights the challenges associated with the use of *in vitro* data to predict *in vivo* performance. It illustrates the value of scintigraphy for understanding the relative *in vivo* performance among different CR formulations, especially when the properties of these formulations are very different.

The *in vivo* erosion rates for all radiolabeled formulations are consistent with exposure data (AUC and C_{\max}) (Fig. 6). The dose-normalized AUC for Compound 645838 continued to increase as the time for complete erosion decreased. Prototype 3 (25 mg) had plasma concentration-time profiles for both LY545694 and Compound 645838 comparable to the profiles achieved with the unlabeled reference CR formulation (35 mg strength). The relative bioavailability for compound 645838 was 30% higher than the unlabeled

reference CR formulation. Among the three prototypes, Prototype 3 achieved the goal of obtaining comparable PK profile (similar AUC and C_{\max}) at a lower dose compared to the reference CR formulation. The C_{\max}/C_{12h} ratio was 19% higher for Prototype 3 compared to the unlabeled reference CR formulation, as expected due to the faster release rate of Prototype 3 (Table II). The increase was considered an acceptable compromise while achieving the desired PK profile.

Investigations of the correlation between scintigraphy data and exposure suggested that delivery to more distal regions (i.e., colonic rather than small intestine) resulted in reduction in the extent of absorption. Furthermore, the time taken to transit through the GI tract also influenced the extent of absorption. Individuals who exhibited longer gastric residence times, and hence had greater opportunity for prodrug delivery to the most conducive absorption sites (duodenum and jejunum), had higher Compound 645838 exposure. These data permit an understanding of the multiple drivers of variability among subjects. In simplistic terms, the more quickly the tablet eroded, the earlier in the GI tract delivery should occur – which should yield the higher exposures. However, this was not always the case. In fact, no overall trend was observed when comparing time taken to erode ($t_{90\%}$) with AUC. As example for the radiolabeled CR reference, subject 13 exhibited the highest exposure. However, the time for complete tablet erosion ($t_{90\%}=4.09$ h) was very close to average value for this group ($t_{90\%}=4.01$ h). The high exposure was actually a result of the dosage form remaining in the stomach for the duration of erosion. Similarly, for prototype 3, two subjects (6 and 13) were

observed to have the highest AUC values and their gastric residence times were the longest observed within the group (> ~2.5 h). In this group, the subjects with the lowest AUC (subjects 5 and 9) had the shortest gastric residence.

An assessment of the metabolite to parent ratio (MTP(%)) in relation to delivery site indicated that conversion to active moiety was reduced when delivery occurred more distally in the GI tract. These data suggest regional differences for conversion in addition to absorption. Overall, the study data support the hypothesis that both the formulation (rate of erosion) and individual GI transit times will impact the rate and extent of absorption.

CONCLUSIONS

A pharmacoscintigraphic study designed as a single adaptive design space study led to the identification of an optimal CR formulation in a clinically-efficient manner. The optimal CR formulation provided comparable Compound 645838 exposure to the reference CR formulation with 30% less drug in the dosage form. Scintigraphy results complemented the PK results and enabled a better understanding of the differences in the *in vivo* performance among the CR formulations tested and allowed efficient decision making. This outcome would have taken multiple iterative studies under a more traditional approach.

ACKNOWLEDGMENTS AND DISCLOSURES

The authors would like to acknowledge the support from Nick McEntee, Abigail Pedigo, Chad Martinsen and Claudia Jacobs for their formulation development and manufacturing support; Matthew Deverall, for providing analytical *in vitro* dissolution support; Robert Stratford for providing clinical analytical support; Shobha Reddy, Chris Payne, Harry Haber (i3 Statprobe, Inc., Ann Arbor MI), and Matt Dunn for their support on the clinical study; Matthew Curley, Gaetan Rygaert, and Stacy Nolan for their quality oversight; and Xuan Ding, for her pre-formulation modeling support.

This work was funded by Eli Lilly and Company.

REFERENCES

- Davis SS, Hardy JG, Fara JW. Transit of pharmaceutical dosage forms through the small intestine. *Gut*. 1986;27:886–92.
- Casey D, Beihn R, Digenis G, Shambu M. Method for monitoring hard gelatine capsule disintegrating times in humans using external scintigraphy. *J Pharm Sci*. 1976;65:1412–3.
- Coupe A, Davis S, Wilding I. Variation in gastrointestinal transit of pharmaceutical dosage forms in healthy subjects. *Pharm Res*. 1991;8(3):360–4.
- Wilding A, Coupe J, Davis S. The role of γ -scintigraphy in oral drug delivery. *Adv Drug Deliv Rev*. 2001;46(1–3):103–24.
- Connor AL, Wray H, Cottrell J, Wilding IR. A scintigraphic study to investigate the potential for altered gut distribution of loperamide from a loperamide-simethicone formulation in man. *Eur J Pharm Sci*. 2001;13(4):369–74.
- Cole E, Scott R, Connor A, Wilding I, Petereit H, Schminke C, *et al*. Enteric coated HPMC capsules designed to achieve intestinal targeting. *Int J Pharm*. 2002;231(1):83–95.
- Katsuma M, Watanabe S, Takemura S, Sako K, Sawada T, Masuda Y, *et al*. Scintigraphic evaluation of novel colon-targeted delivery system (CODES) in healthy volunteers. *J Pharm Sci*. 2004;93(5):1287–99.
- Basit A, Podczeczek F, Newton JM, Waddington W, Ell P, Lacey L. The use of formulation technology to assess regional gastrointestinal drug absorption in humans. *Eur J Pharm Sci*. 2004;21(2):179–89.
- Davis J, Burton J, Connor AL, MacRae R, Wilding IR. Scintigraphic study to investigate the effect of food on a HPMC modified release formulation of UK-294,315. *J Pharm Sci*. 2009;98(4):1568–76.
- Liu F, Lizio R, Meier C, Petereit H, Blakey P, Basit A. A novel concept in enteric coating: a double-coating system providing rapid drug release in the proximal small intestine. *J Control Release*. 2009;133(2):119–24.
- Pahwa R, Dutt H, Kumar V, Kohli K. Pharmacoscintigraphy: an emerging technique for evaluation of various drug delivery systems. *Arch Appl Sci Res*. 2010;2(5):92–105.
- Kwiatek MA, Menne D, Steingoetter A, Goetze O, Forras-Kaufman Z, Kaufman E, *et al*. Effect of meal volume and caloric load on postprandial gastric function and emptying: studies under physiological conditions by combined fiber-optic pressure measurement and MRI. *Am J Physiol Gastrointest Liver Physiol*. 2009;297(5):G894–901.
- Cole E, Scott R, Cade D, Connor A, Wilding I. *In vivo* and *in vitro* pharmacoscintigraphic evaluation of ibuprofen hypromellose and gelatin capsules. *Pharm Res*. 2004;21(5):793–8.
- Davis S, Khosla R, Wilson C, Washington N, Leslie S, Malkowska S. The gastrointestinal transit of a controlled release formulation of indomethacin. *Int J Pharmaceutics*. 1990;60:191–6.
- Wilding I, Davis S, Sparrow R, Smith K, Sinclair K, Smith A. The evaluation of an enteric coated naproxen tablet formulation using scintigraphy. *Eur J Pharm Biopharm*. 1993;39(4):144–7.
- Pham A, Lee P. Probing the mechanisms of drug release from hydroxypropylmethyl cellulose matrices. *Pharm Res*. 1994;11(10):1379–84.
- Gao P, Skoug J, Nixon P, Ju TR, Stemm N, Sung KC. Swelling of hydroxypropyl methylcellulose matrix tablets: 2. Mechanistic study of the influence of formulation variables on matrix performance. *1996;85(7): 732–40*.
- Siepmann J, Peppas N. Modeling of drug release for delivery systems based on hydroxypropyl methylcellulose (HPMC). *Adv Drug Deliv Rev*. 2001;48(2–3):139–57.
- Ghimire M, Hodges L, Band J, O'Mahony B, McInnes F, Mullen A, *et al*. *In-vitro* and *in-vivo* erosion profiles of hydroxypropylmethylcellulose (HPMC) matrix tablets. *J Control Release*. 2010;147(1):70–5.
- Ghimire M, Hodges L, Band J, Lindsay B, O'Mahony B, McInnes F, *et al*. Correlation between *in vitro* and *in vivo* erosion behaviour of erodible tablets using gamma scintigraphy. *Eur J Pharm Biopharm*. 2011;77(1):148–57.
- Skoug JW, Mikelsons MV, Vigneron CN, Stemm NL. Qualitative evaluation of the mechanism of release of matrix sustained release dosage forms by measurement of polymer release. *J Controlled Release*. 1993;27(3):227–45.